Eur. Phys. J. B **21**, 425–435 (2001)

THE EUROPEAN PHYSICAL JOURNAL B

EDP Sciences

Semiclassical theory of integrable and rough Andreev billiards

W. Ihra[1,a], M. Leadbeater[1,2], J.L. Vega[1], and K. Richter[1]

[1] Max-Planck-Institut für Physik komplexer Systeme, Nöthnitzer Straße 38, 01187 Dresden, Germany
[2] Dipartimento di Física, Universitá di Roma III, Via della Vasca Navale 84, 00146 Roma, Italy

Received 21 August 1999 and Received in final form 21 March 2001

Abstract. We study the effect on the density of states in mesoscopic ballistic billiards to which a superconducting lead is attached. The expression for the density of states is derived in the semiclassical S-matrix formalism shedding light onto the origin of the differences between the semiclassical theory and the corresponding result derived from random matrix models. Applications to a square billiard geometry and billiards with boundary roughness are discussed. The saturation of the quasiparticle excitation spectrum is related to the classical dynamics of the billiard. The influence of weak magnetic fields on the proximity effect in rough Andreev billiards is discussed and an analytical formula is derived. The semiclassical theory provides an interpretation for the suppression of the proximity effect in the presence of magnetic fields as a coherence effect of time reversed trajectories. It is shown to be in good agreement with quantum mechanical calculations.

PACS. 05.45.-a Nonlinear dynamics and nonlinear dynamical systems – 74.50.+r Proximity effects, weak links, tunneling phenomena, and Josephson effects – 74.80.Fp Point contacts; SN and SNS junctions

1 Introduction

A superconductor in proximity to a normal conductor affects the spectral density of quasiparticle excitations in the conductor. Recent technological advances in building very clean conductors of mesoscopic size have led to consider this proximity effect not only in the dirty disorder limit, where it is known to play an important role in many transport properties [1–4], but also in ballistic mesoscopic samples [5–8] in proximity to a bulk superconductor. These systems are often modelled by ballistic billiards. Billiard shaped structures connected to a superconductor have been coined Andreev billiards [9]. It was shown in [5,6] that the form of the quasiparticle excitation spectrum in the Andreev billiard depends crucially on whether its classical dynamics is integrable or chaotic. A semiclassical interpretation of these results based on the Eilenberger Green's function [11] was given in [7]. The semiclassical approach has also been extended to mesoscopic samples with a mixed classical phase space [8] and with classical anomalous diffusion [10].

The aim of this contribution is twofold: We first present a derivation of the semiclassical result for the quasiparticle excitation spectrum based on the semiclassical scattering matrix approach as pioneered by Smilansky and co-workers [12,13] which allows for a transparent physical interpretation of the result of [7] in terms of multiple Andreev scattering events [14]. Secondly, we discuss a number of features of the quasiparticle excitation spectrum in an integrable square billiard and in a square billiard with surface roughness. These features include the saturation of the quasiparticle excitation spectrum in the square billiard and a semiclassical explanation of the effect a weak magnetic field has on the quasiparticle excitation spectrum in billiards with surface roughness.

The semiclassical expression for the quasiparticle density of states will be derived in Section 2. The strength of this approach lies in the fact that it allows to see on which level approximations enter semiclassically. The semiclassical theory of chaotic Andreev billiards predicts an exponential suppression of the density of states near the Fermi energy [7,8]. In contrast a random matrix modelling [5,6] leads to the result of a gap in the density of states in an energy interval above the Fermi energy. The scattering matrix approach elucidates one possible origin of the differing results.

In Section 3.1 we discuss the quasiparticle excitation spectrum of a square Andreev billiard in detail. While previous papers concentrated on the linear rise of the spectrum above the Fermi energy [5–7] we focus on the saturation of the excitation spectrum at higher energies. We show that the saturation can be related to the probability distribution of short classical paths hitting the superconducting parts of the billiard boundaries. In Section 3.2 we discuss results for square billiards with additional surface roughness. Surface roughness is modelled as isotropic scattering of electrons and holes from the normal parts of the billiard boundary. An exponential suppression of

[a] e-mail: ihra@physik.uni-freiburg.de

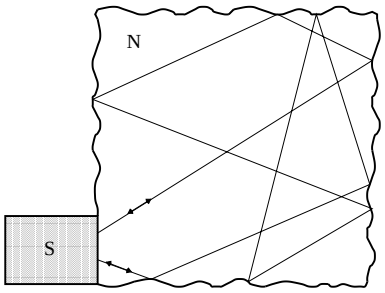

Fig. 1. Square billiard with rough boundaries. Roughness is modelled by isotropic scattering when an electron or hole hits the normal billiard boundary (reflection in any direction with equal probability) in contrast to specular reflection at a smooth boundary. At the SN boundary electrons are retro-reflected (Andreev reflected) as holes and *vice versa*.

the density of states near the Fermi energy is observed in complete analogy to chaotic billiards [8]. Finally in Section 3.3 the effect of an additional weak magnetic field on the quasiparticle excitation spectrum in the rough billiard is considered. We predict an enhanced density of states compared to the field free case for energies near $E_{\rm F}$ and give analytical semiclassical expressions. The semiclassical theory provides a clear interpretation of this result as an effect of destructive interference between reversed paths in the presence of a magnetic field. Again the semiclassical predictions are in good agreement with quantum mechanical calculations.

2 Theory

In a quasi-classical picture the effect of a superconducting lead coupled to a mesoscopic billiard manifests itself in the process known as Andreev reflection [14]: At the superconducting parts of the billiard boundary electron-like quasi-particles are retro-reflected with opposite velocities as holes and *vice versa* (see Fig. 1, and Refs. [4,15] for a detailed description). In contrast electrons and holes are specularly reflected at those parts of the billiard boundary which are not in contact to the superconductor if the billiard boundary is smooth. For a billiard with surface roughness we will take the possibility of isotropic scattering off the normal walls of the billiard into account. This is also indicated in Figure 1.

The local quasiparticle density of states (DOS) $d(E,\mathbf{r})$ of an Andreev billiard is defined as the density of states at positive energy E above the Fermi energy $E_{\rm F}=0$, weighted with the corresponding electron-like component of the wave function at point $\mathbf{r}$. It is given by [7]

$$d(E,\mathbf{r}) = \frac{d_N}{A}\int_0^\pi \mathrm{d}\phi \sum_n \delta\left(\frac{EL(\phi)}{\hbar v_{\rm F}} - (n+\frac{1}{2})\pi\right). \quad (1)$$

A denotes the area of the billiard and $v_{\rm F}$ denotes the Fermi velocity. It is assumed that E is much smaller than the pair potential $\Delta(\mathbf{r})$ in the superconducting lead and that the lead supports a large number $N \gg 1$ of classically allowed transverse channels. In the billiard the pair potential $\Delta(\mathbf{r})$, which couples electron and hole like states, vanishes identically. Due to the condition $E \ll \Delta$ electrons in the billiard which hit the superconducting lead get reflected as holes thus quantum mechanically forming electron-hole quasiparticle states. $L(\phi)$ is the length of the trajectory which passes the point $\mathbf{r}$ in the billiard under an angle ϕ between two successive bounces with the superconducting boundary and $d_N = mA/(2\pi\hbar^2)$ is the average density of states in the isolated billiard. We further assume a perfectly transmitting boundary between the billiard and the lead if the lead is in the normal state (no potential difference), which has the effect that the probability for Andreev reflection equals one if the lead is in the superconducting state. (A situation including the probability for Andreev reflection as well as normal reflection between SN boundaries was taken into account in a somewhat different context and geometry *e.g.* in [16,17].)

The total quasiparticle DOS in the billiard is obtained by integrating (1) over the area of the billiard system. The integral over the billiard area can be converted into an integral over initial starting angles α and positions y of trajectories along the lead of width w. The resulting expression is

$$d(E) = \frac{d_N}{A}\int_0^w \mathrm{d}y \int_{-1}^1 \mathrm{d}(\sin\alpha) \times \int_0^{L(y,\alpha)} \mathrm{d}s \sum_{n=0}^\infty \delta\left(\frac{EL(y,\alpha)}{\hbar v_{\rm F}} - (n+\frac{1}{2})\pi\right), \quad (2)$$

where s is the local variable measuring the length along a trajectory. If one additionally assumes an ergodic distribution of trajectories in the initial conditions y and $\sin\alpha$ on the boundary the expression for the density of states can be rewritten in terms of the probability distribution $P(L)$ of trajectories of length L between two successive bounces with the SN boundary. It is then [7,8]

$$d(E) = \frac{2d_N w}{A}\int_0^\infty \mathrm{d}L\, P(L)\, L \sum_n \delta\left(\frac{EL}{\hbar v_{\rm F}} - (n+\frac{1}{2})\pi\right). \quad (3)$$

The assumption of an ergodic distribution is justified in the case of rough billiards when the time $t_{\rm erg}$ on which the classical motion in the billiard becomes ergodic is much smaller than the mean escape time $\tau_{\rm esc}$ of a particle from the billiard into the SN-lead. It is also a good approximation for the integrable square billiard with a large number of open channels $N \gg 1$ because then the distribution of initial conditions in $\sin\theta$ is quasi-continuous. For a small number of channels it is more appropriate to resort to the continued fraction evaluation of (2) described in Section 3.1, which takes the quantization of angles explicitly into account.

We now aim to derive (3) from the semiclassical scattering matrix approach for quantisation [13] and to understand the approximations which lead to (3) on the

semiclassical level. The scattering matrix approach for quantisation of a billiard system which is opened *via* a lead starts with a trace formula for the density of states $d(E)$ which involves two contributions: The first term $d_{\rm R}(E)$ is the resonance density of states in the corresponding billiard opened *via* the lead. The second contribution takes the coupling to the superconductor into account and is expressed as a sum over traces of powers of the scattering matrix which relates incoming and outgoing transverse modes in the lead. The result is:

$$d(E) = d_{\rm R}(E) - \frac{1}{\pi}\lim_{\eta\to 0}{\rm Im}\frac{\partial}{\partial E}\ln\det\left[1 - S_{\rm A}S_{\rm N}(E+{\rm i}\eta)\right] \tag{4}$$

where the total scattering matrix for the Andreev billiard is composed of a product of a $2N$ times $2N$ normal scattering matrix $S_{\rm N}(E)$ and an Andreev scattering matrix $S_{\rm A}$ of equal dimension. The two scattering matrices are given as [18]

$$S_{\rm N}(E) = \begin{pmatrix} S(E) & 0 \\ 0 & S^*(-E) \end{pmatrix}$$
$$\text{and} \qquad S_{\rm A} = \begin{pmatrix} 0 & -{\rm i} \\ -{\rm i} & 0 \end{pmatrix}. \tag{5}$$

The normal scattering matrix $S_{\rm N}$ has block diagonal structure where the two N times N blocks describe electron and hole scattering between the channel modes. The Andreev scattering matrix $S_{\rm A}$ couples electrons and holes at the SN-interface. The sub-diagonal elements are N times N unit matrices with an additional phase of $(-i)$. We neglect the weak energy dependence of the Andreev scattering matrix which is valid in the deep sub-gap regime $E \ll \Delta$ [15,21]. In terms of the electron and hole scattering matrix the density of states takes the form

$$d(E) = d_{\rm R}(E) - \frac{1}{\pi}{\rm Im}\sum_{m=1}^{\infty}\frac{(-1)^m}{m}{\rm Tr}\frac{\partial}{\partial E}\left[S(E)S^*(-E)\right]^m , \tag{6}$$

where (4) has additionally been expanded into a sum over traces of powers of the scattering matrix. An averaged density can be obtained by different procedures: One can average $d(E)$ over a classically small interval of Fermi energies $E_{\rm F}$ or one can average $d(E)$ over different realizations of the rough billiard (with fixed area A). In any case averaging of the resonance density gives the average density d_N of the isolated billiard, and the average quasiparticle density is

$$d_{\rm av}(E) = d_N(E) - \frac{1}{\pi}{\rm Im}\sum_{m=1}^{\infty}\frac{(-1)^m}{m}{\rm Tr}\frac{\partial}{\partial E}\langle\left[S(E)S^*(-E)\right]^m\rangle . \tag{7}$$

Averaging is denoted by brackets $\langle\cdots\rangle$. Equation (7) is the starting point for the derivation of expression (3) within the semiclassical scattering matrix approach.

Semiclassically the elements $S_{nn'}(E)$ of the electron scattering matrix are expressed as a sum over classical orbits. Each orbit contributes with an amplitude A_j and a phase S_j. The resulting expression is [12,20]

$$S_{nn'}(E) = \sum_j A_j(n\to n')\exp\left[\frac{\rm i}{\hbar}S_j(E,n\to n') - {\rm i}\frac{\pi}{2}\nu_j\right] , \tag{8}$$

where ν_j is an additional integer Maslov index. The amplitude pre-factor is given explicitly by

$$A_j(n\to n') = \left(\frac{\hbar}{2\pi}\right)^{1/2}\left|\frac{\partial I'(E)}{\partial\theta}\right|^{-1/2} \tag{9}$$

where $I' = \hbar n'$ is the action of the final transverse motion in the lead. Only those paths contribute which enter the billiard at the SN-boundary with fixed quantised angle $\pm\sin\theta = n\pi/(k_{\rm F}w)$ and return to the boundary with angle $\pm\sin\theta' = n'\pi/(k_{\rm F}w)$. In terms of the initial position y along the SN boundary and the angle θ' with which the trajectory returns the amplitude can be written as

$$A_j(n\to n') = \frac{1}{w}\sqrt{\frac{\pi}{2k_F}}\left|\frac{\partial y}{\partial(\sin\theta')}\right|^{1/2} . \tag{10}$$

To proceed further we resort to the physical picture of Andreev reflection of electrons into holes and *vice versa* at the SN-boundary. We first observe that the traces contain products of alternating electron scattering matrices $S(E)$ and hole scattering matrices $S^*(-E)$. The energy E above the Fermi level is large with respect to the mean level density $\delta \equiv d_N^{-1}$ of the isolated billiard, but is classically small. Similar to the semiclassical evaluation of density-density correlator [31–33] we expand the phase around the Fermi energy as $S_j(\pm E) \simeq S_j(0) \pm ET_j(0)$ where T_j is the return time of the orbit to the SN-interface. Additionally the amplitudes are only slowly varying functions of the energy and are evaluated at the Fermi energy.

We demonstrate how to evaluate the sum over traces of products of the scattering matrices for the $n = 1$ term. Generalisation to higher order terms is straightforward. Matrix elements of products of an electron and a hole scattering matrix have the form

$$\left[S(E)S^*(-E)\right]_{nn'} = \sum_{n''}\sum_{j,k}A_j(n\to n'')A_k^*(n''\to n') \times\exp\left[\frac{\rm i}{\hbar}(S_j - S_k)\right]\exp\left[\frac{\rm i}{\hbar}E(T_j + T_k)\right]. \tag{11}$$

Upon averaging $\left[S(E)S^*(-E)\right]_{nn'}$ over the Fermi energy or different realizations of boundary roughness in the case of rough billiards only diagonal terms $j = k$ are assumed to contribute to the sum. The diagonal approximation is further justified by the physical picture of Andreev reflection, which means that the reflected hole orbit retraces the electron orbit and *vice versa*. However it must be emphasised that Andreev reflection is exactly fulfilled only at the Fermi energy $E_{\rm F} = 0$, and in an exact treatment

deviations from Andreev reflection at finite energies must be taken into account.

The diagonal approximation implies that the initial and final channel indices are equal, $n = n'$, and the product matrix (11) is diagonal:

$$[S(E)S^*(-E)]_{nn'} = \delta_{nn'} \sum_{n''} \sum_j |A_j(n \to n'')|^2 \exp\left(2\frac{\mathrm{i}}{\hbar} E T_j\right). \quad (12)$$

In the semiclassical limit the summation over intermediate channels n'' can be transformed into an integral over angles: $\sum_{n''} k_\mathrm{F} w/\pi \int_{-1}^{1} \mathrm{d}(\sin\theta')$. Using the expression (10) for the amplitudes one arrives at the final expression

$$[S(E)S^*(-E)]_{nn'} = \delta_{nn'} \frac{1}{2w} \int_0^w \mathrm{d}y \exp(2\frac{\mathrm{i}}{\hbar} E T(y)). \quad (13)$$

Taking the trace amounts to another integration over the angle in the semiclassical approximation and one has

$$\mathrm{Tr}[S(E)S^*(-E)] = \frac{k_\mathrm{F}}{2\pi} \int_{-1}^{1} \mathrm{d}(\sin\theta) \int_0^w \mathrm{d}y \exp(2\frac{\mathrm{i}}{\hbar} E T(y)). \quad (14)$$

Within the diagonal approximation traces of higher powers of products of electron and hole scattering matrices are easily shown to be

$$\mathrm{Tr}[S(E)S^*(-E)]^m = \frac{k_F}{2\pi} \int_{-1}^{1} \mathrm{d}(\sin\theta) \int_0^w \mathrm{d}y \exp(2\frac{\mathrm{i}}{\hbar} m E T(y)). \quad (15)$$

Using the trace formula (7) this gives

$$d_{av}(E) = d_N + \frac{k_\mathrm{F}}{2\pi^2\hbar} \sum_{m=1}^{\infty} (-1)^m \times \int_0^w \mathrm{d}y \int_{-1}^{1} \mathrm{d}(\sin\theta) T \cos(\frac{2mT}{\hbar} E). \quad (16)$$

If now Poisson summation is used the equivalence of (16) and the Bohr-Sommerfeld like expression (2) for the average density of states in the Andreev billiard, which was derived on the basis of the Eilenberger equation for the Green's function [5], can easily be seen.

The scattering matrix approach gives a clear and intuitive interpretation of how the coupling of the billiard to superconducting leads modifies the average density of states: It is given as a sum of the average density of states of the isolated billiard (the Weyl term) plus a sum of multiple Andreev reflections of electron into hole states. The neglection of off-diagonal contributions in the semiclassical approach is a possible explanation for the difference between the random matrix result for a chaotic Andreev billiard [5,6], which predicts a gap in the quasiparticle excitation spectrum for billiards with a chaotic classical phase space, and the semiclassical theory which leads to an exponential suppression [7,8]. Pairs of nonidentical trajectories $k \neq j$ which follow the same path along a segment in real space before they depart due to slightly different initial conditions have similar actions and therefore also survive the averaging of products of electron and hole scattering matrices, equation (11) and powers of it [22]. For systems with ballistic disorder an extended diagonal approximation which takes into account the contribution of paths which are not exactly related by time-reversal symmetry has recently been proposed in the context of weak localisation [23,24] and Andreev billiards [25]. Corresponding off-diagonal pairs of paths also exist in clean (disorder free) chaotic systems. In semiclassical approaches beyond the diagonal approximation these off-diagonal contributions yield random matrix contributions to the spectral form factor [27] and explain weak localization in clean chaotic cavities [28]. The influence of such off-diagonal contributions arising in the semiclassical approach to the density of states in Andreev billiards is presently under investigation.

Finally it should be emphasised that averaging has been performed on classically small scales. Fluctuations of $d_\mathrm{av}(E)$ can still appear on classical energy scales due to fluctuations in the length distribution probability $P(L)$. In the following we will skip the index. $d(E)$ then also denotes the density of states after the above described averaging.

3 Results

In the following we present results of quantum mechanical calculations for the average density of states in Andreev billiards and compare them with the semiclassical theory. We will focus on the difference between results for a square billiard which is integrable and a square billiard with rough boundaries. As an effect of rough boundaries electron and hole trajectories can be scattered into arbitrary directions when they hit the normal boundary. We will then consider the effect of a weak magnetic field on the density of states and derive a semi-analytical expression for the magnetic flux and energy dependence of the density of states.

To numerically model the structure of Figure 1 we consider a ballistic normal region connected to a clean superconductor. For our numerical calculation we use a tight-binding version of the Bogoliubov-de Gennes Hamiltonian:

$$\begin{pmatrix} H_0 & \Delta \\ \Delta^* & -H_0 \end{pmatrix} \begin{pmatrix} u \\ v \end{pmatrix} = E \begin{pmatrix} u \\ v \end{pmatrix}. \quad (17)$$

In this equation $H_0 = \sum_i |i\rangle \epsilon_i \langle i| - t \sum_{\langle ij \rangle} |i\rangle\langle j|$ is the standard single–particle Anderson model with $\langle ij \rangle$ denoting pairs of nearest neighbour sites and $\Delta = \sum_i |i\rangle \Delta_i \langle i|$ is the superconducting order parameter. The billiard has width M and length L (in units of the lattice constant a). The coupling to the superconductor is of width w. With the exception of the billiard boundary, the diagonal matrix elements $\epsilon_i = \epsilon_0$, with ϵ_0 chosen to ensure that the Fermi

level is away from the van Hove singularity in the band centre ($\epsilon_0 = 0$). To model the boundary roughness, for sites on the boundary we randomly choose $\epsilon_i = 10^4$ or $\epsilon_i = \epsilon_0$ with equal probability. In the absence of a magnetic field, the off-diagonal matrix elements t, which determine the width of the energy band (the band-width is $8t$), are set to 1 throughout the system. The effects of a magnetic field are modelled by including a Peierls' phase factor into these off-diagonal elements in the billiard region. To compute the density of states, a numerical decimation technique is employed [29]. This has been used extensively over recent years to discuss transport and density of states properties of hybrid systems [30].

3.1 Square billiards

The asymptotic length distribution of trajectories in square billiards typically follows a power law of the form $P(L) \sim L^{-3}$. This result was used in [5] to show that the density of quasiparticle states is a linear function of the energy of quasiparticle excitations for $E \ll \Delta$. The slope of the linear behaviour is related to the proportionality constant of the asymptotic length distribution. The above distribution however leads to a linear growth of the density of states at all energies and cannot reproduce the large energy limit $d(E) \to d_N$ for the quasiparticle density. We show that the crossover to d_N is related to a modified length distribution $P(L)$ for small lengths. For widths w of the superconducting channel much smaller than the length a of the billiard the length distribution reaches approximately a plateau for small lengths. We introduce two different length distribution functions and compare numerical results to the analytical results derived from the smooth length distribution functions.

It is useful to express the density of states in terms of scaled lengths and energies. Introducing the lengths $L_\mathrm{T} = \pi A/w$ and $E_\mathrm{T} = \hbar v_\mathrm{F}/(2L_\mathrm{T})$ which are sometimes referred to as the Thouless length and the Thouless energy [5–7], lengths $l = L/L_\mathrm{T}$ and energies $\epsilon = E/E_\mathrm{T}$ are expressed in terms of these units. The meaning of L_T and E_T will become clear for chaotic billiards (Sect. 3.2), where L_T is the average length of trajectories before they escape from the billiard. We use the same units of length and energy for the integrable square billiard in order to compare results with the rough billiard later. Expressed in scaled quantities the density of states has the form

$$\frac{d(\epsilon)}{d_N} = \pi \int_0^\infty \mathrm{d}l P(l) l \sum_{n=0}^{\infty} \delta\left(\frac{\epsilon l}{2} - (n+\frac{1}{2})\pi\right) \tag{18}$$

or equivalently

$$\frac{d(\epsilon)}{d_N} = \frac{(2\pi)^2}{\epsilon^2} \sum_{n=0}^{\infty} (n+\frac{1}{2}) P(l_n)\,. \tag{19}$$

We introduce two different length distribution functions. The first length distribution function $P_\mathrm{c}(L)$ approximates the probability by a constant for lengths $l < l_\mathrm{c}$:

$$P_\mathrm{c}(l) = \begin{cases} C_\mathrm{c}/l_c^3 & l < l_\mathrm{c} \\ C_\mathrm{c}/l^3 & l \geq l_\mathrm{c} \end{cases}. \tag{20}$$

The second distribution function has a smooth crossover to a constant probability at small l:

$$P_\mathrm{s}(l) = \frac{C_\mathrm{s}}{l^3 + l_\mathrm{s}^3}\,. \tag{21}$$

We first discuss the length distribution function $P_\mathrm{c}(l)$. For a given energy ϵ there is a value n_0 in the sum (19) given by $n_0 = \epsilon l_\mathrm{c}/(2\pi) - 1/2$ so that for $n > n_0$ the algebraic tail of the length distribution for $P_\mathrm{c}(l_n)$ applies while for $n < n_0$ $P_\mathrm{c}(l_n)$ is constant. The density of states is

$$\frac{d(\epsilon)}{d_N} = C_\mathrm{c} \frac{(2\pi)^2}{\epsilon^2} \left[\frac{1}{l_c^3} \sum_{n=0}^{n_0-1} (n+\frac{1}{2}) + \frac{\epsilon^3}{(2\pi)^3} \sum_{n=n_0}^{\infty} \frac{1}{(n+\frac{1}{2})^2} \right] \tag{22}$$

which after summation and using the relation between n_0 and ϵ becomes

$$\frac{d(\epsilon)}{d_N} = C_\mathrm{c} \left[\frac{2\pi^2}{l_\mathrm{c}^3 \epsilon^2} \left(\frac{\epsilon l_\mathrm{c}}{2\pi} - \frac{1}{2} \right)^2 + \frac{\epsilon}{2\pi} \psi' \left(\frac{\epsilon l_\mathrm{c}}{2\pi} \right) \right] \quad \text{for} \quad \epsilon > \pi. \tag{23}$$

ψ' is the derivative of the Digamma function. This expression for the spectral density is valid for $\epsilon > \pi$, otherwise $n_0 = 0$ and the first part in the sum does not contribute. For $\epsilon < \pi$ the result is

$$\frac{d(\epsilon)}{d_N} = C_\mathrm{c} \frac{\pi}{4} \epsilon, \tag{24}$$

which shows the known linear behaviour for small energies in square billiards [5]. Using $\psi'(x) \to 1/x$ as $x \to \infty$ the asymptotic behaviour for large energies is given by

$$\frac{d(\epsilon)}{d_N} \to \frac{3C_\mathrm{c}}{2l_\mathrm{c}} \quad \text{as} \quad \epsilon \to \infty. \tag{25}$$

The values of the free parameters are determined by the requirements that (a) the probability distribution must be normalised: $\int_0^\infty P(l)\mathrm{d}l = 1$ and (b) for large excitation energies the influence of the coupling to the superconductor vanishes and thus $d(\epsilon) \to d_N$ as $\epsilon \to \infty$. This gives the values $l_\mathrm{c} = 1$ and $C_\mathrm{c} = 2/3$. It is seen that these requirements automatically determine the proportionality constant C_c of the asymptotic power law tail of the length distribution (20) and thus the slope $C_\mathrm{c}\pi/4$ of the linear behaviour (24) of the low energy spectral density. The value $\pi/6$ is somewhat smaller than the value $2/\pi$ given by the authors of [5] who based their calculations on a numerically observed value of $C = 8/\pi^2$ but did not take a crossover of $P(l)$ to a flat distribution at some value l_c into account. Note that one could adjust C

independently to a given value if one introduced a three parameter function for the length distribution $P(l)$, *i.e.* by giving a cut-off length l_* below which $P(l_*) = 0$. Such a cut-off length parameter would quite naturally be of order $l_* \approx 2a$. We will however not deal with this alternative here as when using a three parameter length distribution probability formulas become rather involved.

The length distribution (20) is easy to handle and gives results which agree well with quantum mechanical calculations. It leads however to an unphysical discontinuity of the derivative of $d(\epsilon)$ at $\epsilon = \pi$. The second length distribution (21) we used is free of this feature. Proceeding in the same way as outlined above the spectral density of quasiparticle states is given by

$$\frac{d(\epsilon)}{d_N} = \frac{C_\mathrm{s}}{2\pi}\epsilon \sum_{n=0}^{\infty} \frac{n+\frac{1}{2}}{\left(\frac{\epsilon l_\mathrm{s}}{2\pi}\right)^3 + \left(n+\frac{1}{2}\right)^3}\,. \tag{26}$$

The requirement of normalisation of $P_\mathrm{s}(l)$ leads to $C_\mathrm{s} = 3\sqrt{3}l_0^2/(2\pi)$. Further evaluation is only possible in the small and large energy limits. The small energy limit ($\epsilon l_\mathrm{s} \ll 2\pi$) gives again the result (24) with C_c replaced by C_s. In the opposite high energy limit the summation can be replaced by integration over the continuous variable $x = 2\pi/(\epsilon l_\mathrm{s})(n+1/2)$, leading to

$$\frac{d(\epsilon)}{d_N} = \frac{C_\mathrm{s}}{l_\mathrm{s}} \int_{x_0}^{\infty} \frac{x}{1+x^3}\mathrm{d}x\,, \qquad x_0 = \frac{\pi}{\epsilon l_\mathrm{s}}, \tag{27}$$

and finally

$$\frac{d(\epsilon)}{d_N} = \frac{C_\mathrm{s}}{\pi}\epsilon\ {}_2F_1\left(\frac{1}{3}, 1, \frac{4}{3}, -\frac{1}{x_0^3}\right) \to \frac{2\pi C_s}{3\sqrt{3}l_0} \quad \text{as} \quad \epsilon \to \infty. \tag{28}$$

The values of the parameters of the length distribution function are given by $l_\mathrm{s} = 1$ and $C_\mathrm{s} = 3\sqrt{3}/(2\pi)$. This value of C is very close to $C = 8/\pi^2$ of [5] giving a slope of $3\sqrt{3}/8 \approx 0.6495$ of $d(\epsilon)/d_N$ for small energies compared to $2/\pi \approx 0.6366$ of [5].

In Figure 2 we present a characteristic example of length distribution probabilities for a small channel width $w \ll a$. A plateau in the length distribution function $P(l)$ for $l < 1$ is clearly visible. Here the crossover from the asymptotic power law for long lengths to the plateau is slightly better modelled by $P_\mathrm{c}(l)$ compared to $P_\mathrm{s}(l)$.

We also calculated the density of states for individual square billiards starting from the semiclassical formula (2) without employing the assumption of an ergodic distribution of initial conditions on the SN-boundary. For individual square billiards this formula is more appropriate than (3) before averaging over Fermi energy since it does not involve the assumption of an ergodic distribution of initial conditions of trajectories on the SN-boundary. In square billiards trajectories with equal length between two hits with the channel lead are organised in families (for a discussion see [34]). Orbits with channel index $a = 1, \cdots, N$ hit the SN-boundary under an angle $\sin\theta_a = a\pi/(k_\mathrm{F}w)$. For each channel a there is a finite

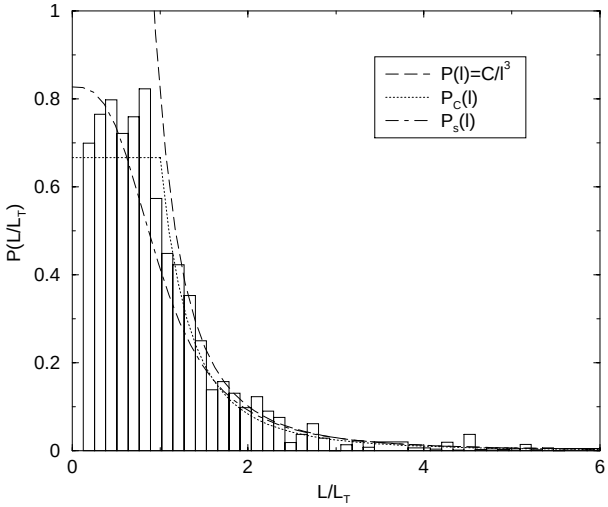

Fig. 2. Histogram of the length distribution probability $P(L/L_\mathrm{T})$ for a square billiard obtained by evaluating equation (29) by the method of continued fractions. Parameters: Length of the billiard sides $a = 1$, width of the superconducting lead $w = 0.1$. The histogram is an average over different numbers of channels ranging from $N = 96$ to $N = 105$. Dashed line: asymptotic power law for large l. Dotted line: $P_\mathrm{c}(l)$, equation (20). Dot-dashed line: $P_\mathrm{s}(l)$, equation (21).

number of orbit families λ_a with different lengths L_{λ_a}. Each member of an orbit family carries a weight δ_{λ_a} with which it contributes to the density of states which is then given by

$$d(E) = \frac{d_N}{A}N^{-1}\sum_{a=1}^{N}\sum_{\{\lambda_a\}}\delta_{\lambda_a}L_{\lambda_a} \times \sum_{n=0}^{\infty}\delta\left(\frac{EL_{\lambda_a}}{\hbar v_\mathrm{F}} - (n+\frac{1}{2})\pi\right) \tag{29}$$

with $\sum_{\{\lambda_a\}}\delta_{\lambda_a} = w$ for the sum of weights of the members λ_a of a single channel a. The lengths L_{λ_a} of contributing trajectory families and their weights δ_{λ_a} can be very efficiently calculated by means of an algorithm involving a finite number of continued fractions as described in [34]. Figure 3 shows the result of a quantum mechanical calculation for a billiard with $w/a = 1/3$ and $N = 12$ channels. The solid line is a 20-point average over the quantum mechanical data. The dashed line represents the semiclassical result obtained from equation (29). It follows the general trend of the quantum mechanical result but is somewhat lower. Also plotted as dotted and dot-dashed lines are the formulas for the averaged quasiparticle excitation spectrum obtained from equations (23, 24) and (26). The linear behaviour of the quasiparticle spectrum for small excitation energies based on the asymptotic length distribution function $P(l)$ without plateau is plotted as the long dashed line. The average of the quantum mechanical result is in good agreement with the results of equations (23, 24) and (26). Both the numerical semiclassical result (dashed line) and the quantum mechanical result show however additionally a pronounced oscillation around the mean value $d(\epsilon) = d_N$ at energies $\epsilon > 1$.

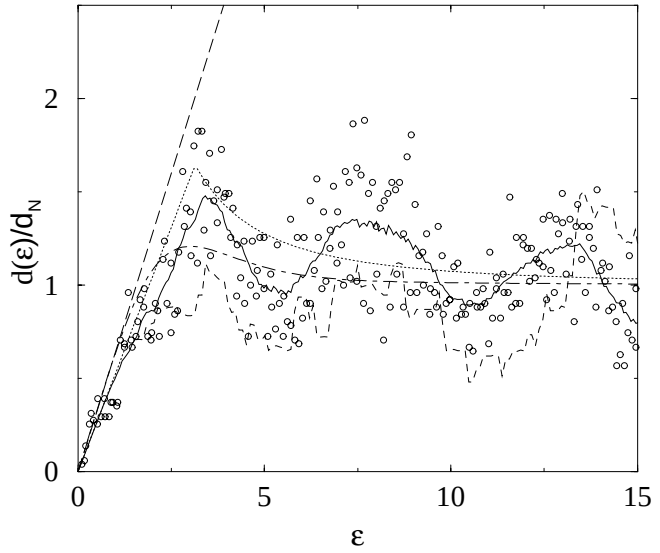

Fig. 3. Average density of states $d(\epsilon)/d_N$ as a function of the energy $\epsilon = E/E_{\rm T}$. The circles are quantum mechanical calculations for a square billiard of side length $a = 75$ and channel width $w = 25$ ($N = 12$). The solid line is a 20-point average over the set of data points. Dashed line: Semiclassical result from equation (29). Dotted line: DOS using $P_{\rm c}(l)$ from equation (20). Dot-dashed line: DOS using $P_{\rm s}(l)$ from equation (21) Long dashed line: Low energy limit $d(\epsilon)/d_N = (2/\pi)\epsilon$ based on the probability distribution $P(l) = C/l^3$.

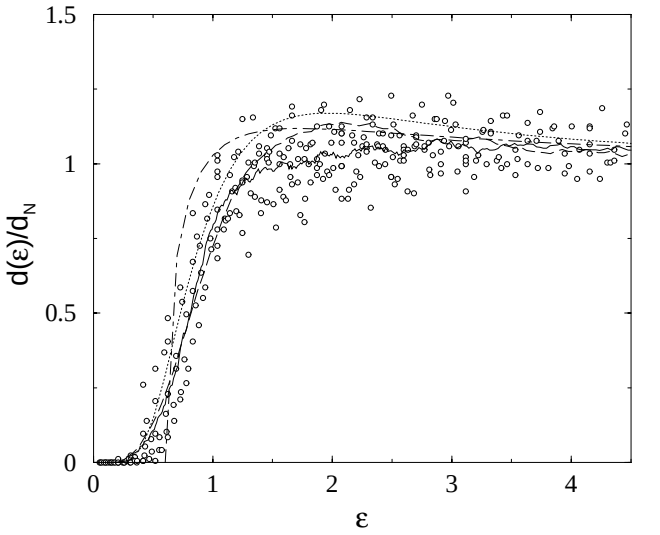

Fig. 4. Average density of states for a rough square billiard. Data points are quantum mechanical energy eigenvalues for a billiard of side length $a = 75$ and channel widths $15 \le w \le 40$ ($7 \le N \le 20$). The solid line is a 20-point average of the numerical data. Dashed curve: semiclassical calculation based on equation (2). Dotted curve: Analytical expression equation (31). Dot-dashed line: Random matrix result of [3].

We observed this trend also for other individual square billiards with different parameter values of w/a and N. The origin of these oscillations has not yet been identified and deserves further investigations.

4 Rough billiards

In this subsection we apply the semiclassical result (3) for the quasiparticle density of states to the square billiard with additional surface roughness. In the following we discuss the situation where the width w of the superconducting channel is much smaller than the length a of one billiard side. Since a trajectory randomises once it hits the rough billiard walls due to off-scattering in arbitrary direction with equal probability the motion becomes ergodic on a time scale much smaller than the mean time between two hits with the superconducting part of the boundary. The latter can also be viewed as the escape time of trajectories from the billiard if it was open along the channel lead. The escape probability $P(L)$ of trajectories of length L from an open chaotic billiard is known to be given asymptotically by [12,35]

$$P(L) = \frac{1}{L_{\rm T}} \exp\left(-\frac{L}{L_{\rm T}}\right) \tag{30}$$

with the above defined Thouless length $L_{\rm T}$ [5]. It is related to the mean escape time by $\tau_{\rm esc} = L_{\rm T}/v_{\rm F}$. Note that averaging over different realizations of the rough billiard is effectively taken into account by the introduction of the smooth length distribution function $P(L)$ by which a probabilistic description on the classical level is achieved. Numerical calculations confirm the form (30) of $P(L)$ for long trajectories. Using (30) the average density of states can be calculated from equation (3) by evaluating the delta function integral directly and summing over n. The result is

$$d(\epsilon) = d_N \left(\frac{\pi}{\epsilon}\right)^2 \frac{\cosh\left(\frac{\pi}{\epsilon}\right)}{\sinh^2\left(\frac{\pi}{\epsilon}\right)} \quad \text{with} \quad \epsilon = \frac{E}{E_{\rm T}}\,,\ E_{\rm T} = \frac{\hbar v_{\rm F}}{2L_{\rm T}}\,. \tag{31}$$

This result was also derived in [8] in the context of a chaotic billiard coupled to a superconducting lead of small width w. It remains valid for billiards with boundary roughness as long as the time scale $t_{\rm erg}$ on which the classical motion in the billiard becomes ergodic is much smaller than the mean escape time $\tau_{\rm esc}$.

The semiclassical prediction (31) is compared with numerical quantum mechanical results in Figure 4. A 20-point average was taken over the numerical results for different channel widths w (solid curve). It is in very good agreement with the analytical formula (31) (dotted curve) as well as an evaluation of equation (3) with numerically calculated length distribution functions $P(L)$ (dashed curve). The Thouless energy is inversely proportional to twice the escape time $\tau_{\rm esc}$ of an electron trajectory since for a complete transversal of a path hitting the SN-boundary the electron part and the retracing as a hole trajectory have to be added for one full cycle.

The exponential suppression of the spectral density for the rough billiard in contrast to the linear rise in energy for

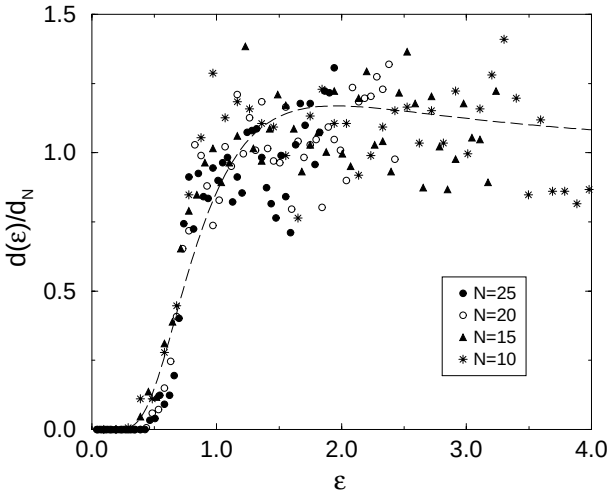

Fig. 5. Density of states for the rough square billiard for different numbers N of open channels. The number of open channels varies as $N = w/2$ with $a = 50$. Dashed curve: Analytical expression equation (31).

the square billiard without roughness has its origin in the asymptotic behaviour of the length distribution function $P(L)$. The density of low-lying quasiparticle excitations is determined by very long orbits in order to fulfill the delta function condition in equation (3) in the limit $E \to 0$. As a consequence of the exponential tail of the length distribution (30) the density of states is exponentially suppressed above the Fermi energy. In contrast the algebraic tail of $P(L)$ in the square billiard without roughness leads only to a linear suppression in energy.

In a different approach the Hamiltonian of an (isolated) chaotic mesoscopic billiard was modelled by a GOE ensemble from random matrix theory and its coupling to the superconducting leads was then taken into account by means of a coupling matrix [5,6]. There it was shown that the quasiparticle density of states vanishes *exactly* below an energy of approximately $E_c < 0.6E_T$ (see dashed-dotted line in Fig. 4). As discussed at the end of Section 2 the difference between the two results may be traced back to the diagonal approximation employed in the semiclassical theory. The quantum mechanical results of Figure 4 are in good agreement with the semiclassical prediction of an exponential suppression of the density of states. This is due to the fact that the random matrix theory of [5] predicts a gap in the excitation spectrum in the limit of an infinity number of channels $N \to \infty$ (since it is essentially an expansion in the parameter $1/N$).

For a finite number of channels the behaviour of the spectral density around E_c is expected to be smoothed out [22,26]. Our quantum mechanical results indicate that the N dependence is weak for the range of N ($10 \le N \le 25$) used in our calculations (see Fig. 5), but they do not allow for a clear-cut determination of the exponent.

4.1 Effect of a magnetic field in rough billiards

In this subsection we consider the effect of a magnetic field on the density of quasiparticle states. The magnetic field B is uniform and points in the direction perpendicular to the billiard area. The superconducting lead itself is not penetrated by the flux. We study the perturbative regime of small magnetic fields where the cyclotron radius is much larger than the length scale a defined by the size of the mesoscopic billiard itself. The trajectories are then unchanged and the only effect of the magnetic field is an additional phase acquired by each trajectory which is proportional to the directed flux enclosed by the trajectory [36]. Formula (2) for the average density of states is then modified to include the flux dependent phase for each trajectory. The result is

$$d(E) = \frac{d_N}{A} \int_0^W \mathrm{d}y \int_{-1}^{1} \mathrm{d}(\sin\alpha) \times \int_0^{L(y,\alpha)} \mathrm{d}s \sum_n \delta\left(\frac{EL(y,\alpha)}{\hbar v_F} - (n+\frac{1}{2})\pi + 2\pi \frac{\Phi(y,\alpha)}{\Phi_0} \right), \tag{32}$$

where $\Phi_0 = ch/e$ is the flux quantum. Electron trajectories which traverse the billiard in opposite directions between two hits with the superconducting part of the boundaries acquire flux of same magnitude but opposite sign [37]. For the generic case of rough or chaotic billiards a statistical description can be used in the same way as was done in the previous section for the magnetic field free case. In addition to the length distribution $P(L)$, which remains unchanged, the distribution $P_L(\Theta)$ of the directed area Θ enclosed by the trajectories of given length L must be specified. For long trajectories it is given by a Gaussian of the form [35,36]

$$P_L(\Theta) = \frac{1}{\sqrt{2\pi L \sigma_L}} \exp\left(-\frac{\Theta^2}{2L\sigma_L} \right), \tag{33}$$

where Θ is the directed area enclosed by the orbit. A heuristic argument for this distribution goes as follows: for a long orbit the length is on average proportional to the number of bounces with the rough billiard walls. At each bounce the trajectory is randomised and therefore the area swept between two successive bounces can be viewed as a random variable with zero mean value. Trajectory segments are independent of each other. The total area Θ accumulated by a trajectory is therefore a sum of independent random variables and its distribution is a Gaussian. It follows that the area distribution integrated over length has an exponential form: $P(\Theta) = (2\bar{\Theta})^{-1} \exp(-\Theta/\bar{\Theta})$ with $\bar{\Theta} = \sqrt{L_T \sigma_L/2}$.

Using the above area distribution and an ergodic distribution of initial conditions along the superconducting

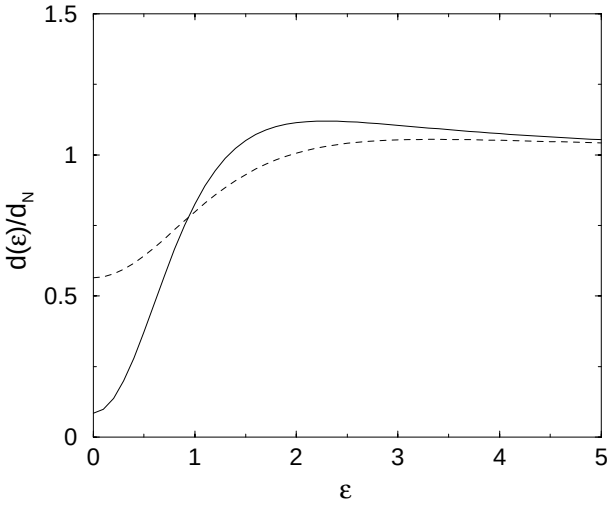

Fig. 6. Average density of states $d(\epsilon)/d_N$ for the rough square billiard of unit area in the presence of a flux according to the semiclassical formula (35). Solid line: $\phi = 0.5$. Dashed line: $\phi = 1.0$.

channel boundary the density of states can be rewritten as

$$d(E,B) = \frac{d_N W}{A}\int_0^\infty \mathrm{d}L\, P(L)\, L \int_{-\infty}^{\infty} \mathrm{d}\Theta P_L(\Theta) \times \sum_n \delta\left(\frac{EL}{\hbar v_\mathrm{F}} - (n+\frac{1}{2})\pi + \frac{2\pi B\,\Theta}{\Phi_0}\right). \quad (34)$$

Transforming the sum over delta functions by use of the Poisson formula and performing the integration over areas and lengths successively one finally gets the following expression for the average spectral density of quasiparticle excitations as a function of energy and magnetic flux:

$$d(\epsilon,\phi) = d_N + 2d_N \sum_{k=1}^{\infty}(-1)^k \frac{(1+k^2\phi^2)^2 - (k\epsilon)^2}{[(1+k^2\phi^2)^2 + (k\epsilon)^2]^2},$$
$$\phi = \frac{4\pi B}{\Phi_0}\sqrt{2\sigma_L L_T}\,. \quad (35)$$

The dimensionless quantity ϕ is the effective flux through the billiard measured in units of the flux quantum $\Phi_0 = ch/e$. This is evident when it is written as $\phi = 4\pi B\bar{\Theta}/\Phi_0$. $\bar{\Theta}$ has the meaning of an effective area. The dimensionless flux can also be expressed as $\phi = \Phi_\mathrm{tot}/\Phi_\mathrm{cr}$, where $\Phi_\mathrm{tot} = BA$ is the total flux through the billiard and $\Phi_\mathrm{cr} = A/(4\pi\bar{\Theta})\Phi_0$. As will be discussed in the following in the regime $\Phi_\mathrm{tot} < \Phi_\mathrm{cr}$ ($\phi < 1$) the exponential suppression of the DOS near the Fermi energy persists while for larger fluxes the DOS converges towards a constant value. Figure 6 shows the quasiparticle excitation spectrum as a function of energy for two different values of the flux parameter ϕ. With growing flux the average density of states acquires the value d_N of the isolated billiard also for values $E < E_\mathrm{T}$.

At the Fermi energy $\epsilon = 0$ equation (35) can be summed and gives

$$d(\epsilon = 0,\phi) = \frac{d_N}{2}\frac{\pi}{\phi}\left[\sinh\frac{\pi}{\phi}\right]^{-1}\left[\frac{\pi}{\phi}\coth\frac{\pi}{\phi} + 1\right]. \quad (36)$$

Equation (36) should not be understood in the sense of an expression for the density of states *exactly* at the Fermi level. Properly interpreted it is *proportional* to the quasiparticle density of states as a function of the magnetic flux when the density of states is averaged over an energy window larger than the mean level spacing δ above the Fermi energy. (Note that the averaging is over an energy scale much smaller than E_T). It has been shown that even at fluxes $\phi \gg 1$ a minigap of order of the mean level spacing is present in the quasiparticle density of states at the Fermi level [18,19]. Therefore the quasiparticle DOS exactly at the Fermi level is always zero. According to reference [18] for a billiard whose isolated dynamics is described by a GUE matrix ensemble (which corresponds to $\phi > 1$) the DOS is given by $d_\mathrm{GUE}(E)/d_N = 1 - \sin(2\pi d_N E)/(2\pi d_N E)$. When $d_\mathrm{GUE}(E)/d_N$ is averaged over the interval $0 < E < \delta$ it gives the value $g = 0.77$. Using this asymptotic value for large fluxes we can approximate the DOS d_δ averaged over the window $0 \le E \le \delta$ semiclassically as

$$d_\delta(0,\phi) \simeq g d(0,\phi)\,. \quad (37)$$

The factor g has the effect that $d_\delta(0,\phi)$ saturates at a value smaller than 1 in large magnetic fields, which is the consequence of the existence of the minigap.

Figure 7 compares the semiclassical prediction of equation (36) and equation (37) (dashed line) with a numerical quantum mechanical calculation (solid line). It shows that $d_\delta(0,\phi)$ is exponentially suppressed on the scale $\phi < 1$. The quantum mechanical results were obtained for a rough billiard (sides $a = 1$ and $b = 1.5$) with 10 different values of the width between $w = 0.2$ and $w = 0.38$. In reference [35] numerical evidence was put forward that the effective area scales like $\bar{\Theta} = \alpha_0 A^{5/4} w^{-1/2}$ with the parameters of the billiard (α_0 is a numerical parameter). The flux scale Φ_cr entering into the magnetic field dependence of the DOS then scales as $\Phi_\mathrm{cr} = (4\pi\alpha_0)^{-1} w^{1/2} A^{-1/4}\Phi_0$. The quantum mechanical calculations for different channel widths w and fixed billiard area A confirm this scaling property. Determining $\alpha_0 = 0.1$ from the numerical data the flux scale Φ_cr is fixed for each value of w. The quantum mechanical data points plotted as a function of the flux $\Phi_\mathrm{tot}/\Phi_\mathrm{cr}$ and its average (solid line) are in excellent agreement with the semiclassical theory of equation (37).

The difference between equation (36) which would lead to a finite density of states at $\epsilon = 0$ at nonzero flux and the exact result of reference [18] which predicts the minigap shows that the semiclassical approximation is not applicable for energies $E < \delta$. As it is known the diagonal approximation, which we employed, breaks down on the scale of the mean level spacing [31,38] and therefore semiclassics within the diagonal approximation does not lead to the correct result on the scale of the mean level spacing itself. When the density of states is averaged over a

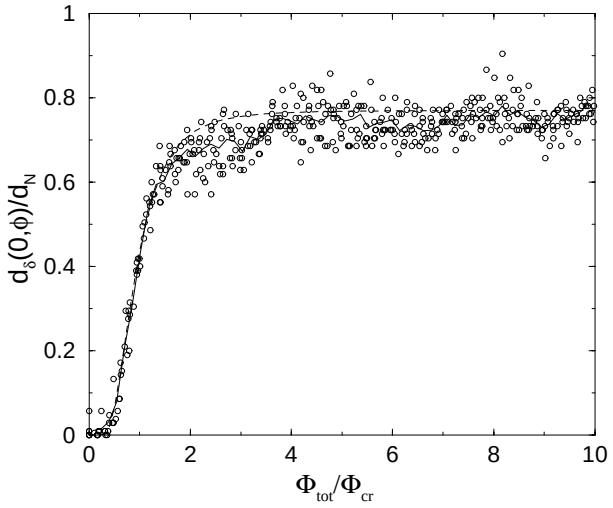

Fig. 7. Spectral density $d_\delta(0,\phi)/d_N$ of quasiparticle excitations as a function of the flux $\phi = \Phi_{\rm tot}/\Phi_{\rm cr}$ for the rough square billiard. The density of states is averaged over the small energy interval $0 \leq E \leq \delta$, where δ is the mean level spacing of the isolated billiard. Data points: quantum mechanical calculation width 10 different channel width w. Solid line: Average over quantum mechanical data points. Dashed line: semiclassical theory, equations (36) and (37).

scale of the mean level spacing δ or larger equation (37) describes the behaviour of the spectral density correctly as discussed above.

Finally we would like to emphasize that the semiclassical theory allows to interpret the destruction of the proximity effect in the presence of a magnetic field as a quantum mechanical interference phenomenon. Classically the return probability of trajectories to the SN-interface is given by $P(L)$. Without magnetic field a path and its reverse interfere constructively. In the presence of a magnetic flux a phase difference between a path and its reverse arises. The quantum mechanical return probability is reduced compared to its classical value $P(L)$ [33]. As a result the DOS of the quasi-particle excitation spectrum is modified compared to the zero field value according to equations (34) and (35).

5 Summary

We studied the quasiparticle excitation spectrum of a mesoscopic conductor modelled by a billiard in proximity to a superconducting lead. The expression for the density of states was derived from the semiclassical scattering matrix formulation. It was shown to be equivalent to the result derived previously from the Eilenberger equation for the quasiparticle Greens function when the diagonal approximation is applied to traces of powers of the scattering matrix. Applications to a square billiard as an example of a classical integrable system and a square billiard with surface roughness as an ergodic system were considered. For the square billiard without roughness it was shown that the deviation of the length distribution function of trajectories hitting the superconducting part of the boundary at small lengths is responsible for the saturation of the average density of states at large energies. For the rough billiard semiclassics predicts an exponential suppression of the density of states at energies smaller than the Thouless energy. The difference to the random matrix result of an energy gap of order of the Thouless energy can be traced back to the diagonal approximation employed in the semiclassical theory. The semiclassical predictions are in good agreement with quantum mechanical calculations for the integrable as well as for the ergodic billiard. Finally we derived expressions for the effect of a weak magnetic field on the density of states in the rough billiard. A magnetic field destroys the proximity effect on the density of states. We interpreted this fact as a phase phenomenon involving identical but reversed paths which hit the superconducting part of the billiard boundary.

We enjoyed discussions with A. Altland, C. Beenakker, K. Frahm, B. Mehlig and H. Schomerus and thank M. Sieber for a critical reading of the manuscript. WI would especially like to thank F. Mota-Furtado and P.F. O'Mahony for encouraging him to work on Andreev billiards and for discussions on the subject in the early stage of this work.

References

1. W.L. McMillan, Phys. Rev. **175**, 537 (1968).
2. A.F. Volkov, Physica B **203**, 267 (1994).
3. W. Belzig, C. Bruder, G. Schön, Phys. Rev. B **54**, 9443 (1996).
4. For a detailed review see C.J. Lambert, R. Raimondi, J. Phys. Cond. Matt. **10**, 901 (1998) and references therein.
5. J.A. Melsen, P.W. Brouwer, K.M. Frahm, C.W.J. Beenakker, Europhys. Lett. **35**, 7 (1996).
6. J.A. Melsen, P.W. Brouwer, K.M. Frahm, C.W.J. Beenakker, Physica Scripta T **69**, 223 (1997).
7. A. Lodder, Yu.V. Nazarov, Phys. Rev. B **58**, 5783 (1998).
8. H. Schomerus, C.W.J. Beenakker, Phys. Rev. Lett. **82**, 2951 (1999).
9. I. Kosztin, D.L. Maslov, P.M. Goldbart, Phys. Rev. Lett. **75**, 1735 (1995).
10. W. Ihra, K. Richter, Physica E **9**, 362 (2001).
11. G. Eilenberger, Z. Phys. **214**, 195 (1968).
12. E. Doron, U. Smilansky, Phys. Rev. Lett. **68**, 1255 (1992).
13. U. Smilansky, in *Mesoscopic Quantum Physics, Les Houches Summer School 1994*, edited by E. Akkermans, G. Montambaux, J.-L. Pichard, J. Zinn-Justin (Elsevier Science B.V., 1995).
14. A.F. Andreev, JETP **19**, 1228 (1964), JETP **22**, 455 (1966).

15. C.W.J. Beenakker, in *Mesoscopic Quantum Physics, Les Houches Summer School 1994*, edited by E. Akkermans, G. Montambaux, J.-L. Pichard, J. Zinn-Justin (Elsevier Science B.V., 1995).
16. B.J. van Wees, P. de Vries, P. Magnée, T.M. Klapwijk, Phys. Rev. Lett. **69**, 510 (1992).
17. A.F. Morpugo, S. Holl, B.J. van Wees, T.M. Klapwijk, G. Borghs, Phys. Rev. Lett. **78**, 2636 (1997).
18. K.M. Frahm, P.W. Brouwer, J.A. Melsen, C.W.J. Beenakker, Phys. Rev. Lett. **76**, 2981 (1996).
19. A. Altland, M.R. Zirnbauer, Phys. Rev. Lett. **76**, 2981 (1996).
20. W.H. Miller, Adv. Chem. Phys. **9**, 48 (1974).
21. C.W.J. Beenakker, Phys. Rev. Lett. **67**, 3836 (1991).
22. K. Frahm, private communication.
23. I.L. Aleiner, A.I. Larkin, Phys. Rev. B **54**, 14423 (1996).
24. R.A. Smith, I.V. Lerner, B.L. Altshuler, Phys. Rev. B **58**, 10343 (1998).
25. D. Taras-Semchuk, A. Altland, preprint `cond-mat/0010413`.
26. M.G. Vavilov, P.W. Brouwer, V. Ambegaokar, C.W.J. Beenakker, Phys. Rev. Lett. **86**, 874 (2001).
27. M. Sieber, K. Richter, Physica Scripta, in press (2001).
28. K. Richter, M. Sieber, unpublished (2001).
29. C.J. Lambert, D. Weaire, Phys. Stat. Sol. (b) **101**, 591 (1980); M. Leadbeater, C.J. Lambert, Ann. Phys. (Leipzig) **7**, 498 (1998).
30. see for example: M. Leadbeater, C.J. Lambert, K. Nagaev, R. Raimondi, A. Volkov, Phys. Rev. B **59**, 12264 (1999); M. Leadbeater, V. Falko, C.J. Lambert, Phys. Rev. Lett. **81**, 1274 (1998); M. Leadbeater, C.J. Lambert, Phys. Rev. B **56**, 826 (1997).
31. M.V. Berry, Proc. Roy. Soc. London Ser. A **400**, 229 (1985).
32. A.M. Ozorio de Almeida, *Hamiltonian Systems: Chaos and Quantization* (Cambridge, New York, 1988).
33. N. Argaman, Y. Imry, U. Smilansky, Phys. Rev. B **47**, 4440 (1993).
34. P. Pichaureau, R.A. Jalabert, Eur. J. Phys. B **9**, 299 (1999).
35. H.U. Baranger, R.A. Jalabert, A.D. Stone, Chaos **3**, 665 (1993).
36. K. Richter, D. Ullmo, R.A. Jalabert, Phys. Rep. **276**, 1 (1996).
37. C. Bruder, Y. Imry, Phys. Rev. Lett. **80**, 5782 (1998).
38. E.B. Bogomolny, J.P. Keating, Phys. Rev. Lett. **77**, 1472 (1996).